

Higgs-radion mixing in stabilized brane world models

Edward E. Boos, Viacheslav E. Bunichev, Maxim A. Perfilov, Mikhail N. Smolyakov,
Igor P. Volobuev

Skobeltsyn Institute of Nuclear Physics, Lomonosov Moscow State University
119991 Moscow, Russia

Abstract

We consider a quartic interaction of the Higgs and Goldberger-Wise fields, which connects the mechanism of the extra dimension size stabilization with spontaneous symmetry breaking on our brane and gives rise to a coupling of the Higgs field to the radion and its KK tower. We estimate a possible influence of this coupling on the Higgs-radion mixing and study restrictions on model parameters from the LHC data.

1 Introduction

In the present paper we consider an extension of the Standard Model (SM) based on the Randall-Sundrum model with two branes stabilized by a bulk scalar field [1, 2, 3, 4], which is necessary for the model to be phenomenologically acceptable. A characteristic feature of this extension is the presence of a massive scalar radion field together with its Kaluza-Klein (KK) tower. These fields have the same quantum numbers as the neutral Higgs field. Thus, the radion field and its excitations can mix with the Higgs field, if they are coupled.

Originally, a Higgs-radion coupling in the unstabilized Randall-Sundrum model arising due to a Higgs-curvature term on the brane was put forward in [5]. Then, such a coupling and the resulting Higgs-radion mixing in the case of the stabilized model were discussed in paper [6] without taking into account the KK tower of higher scalar excitations. The phenomenology of the Higgs-radion mixing originating from the Higgs-curvature term was also considered in view of the discovery of the Higgs-like boson at the LHC [7]; various assumptions about the masses and the mixings of the scalar states have been analyzed in papers [8]–[16]. In particular, it was shown that the light radion-dominated state with mass below or above the observed 125-GeV boson is still not completely excluded by all the electroweak precision constraints and the LHC data.

Here, we discuss a different mechanism of Higgs-radion mixing immanent in stabilized brane-world models, where a Higgs-radion coupling naturally arises due to spontaneous symmetry breaking on the brane involving the stabilizing scalar field. This approach takes into account the influence of the KK tower of higher scalar excitations on the parameters of the Higgs-radion mixing, which turns out to be of importance.

In principle, the most general mechanism of Higgs-radion mixing can include both possible Higgs-radion couplings. However, after the spontaneous symmetry breaking on the brane the Higgs-curvature term also gives rise to a brane-localized curvature term that affects the mass spectrum and the couplings to matter of the graviton KK modes [17]; this effect should be taken into account when examining the four-dimensional effective theory. For this reason, here we restrict ourselves to the new mechanism of Higgs-radion mixing, which has the advantage that it modifies only the scalar sector of the model and leaves intact the masses and the coupling

constants of the graviton KK excitations. This also allows one to isolate the effects due only to the new mechanism of the mixing.

2 Higgs-radion interaction

A stabilized brane-world model in five-dimensional space-time $E = M_4 \times S^1/Z_2$ with coordinates $\{x^M\} \equiv \{x^\mu, y\}$, $M = 0, 1, 2, 3, 4$, $\mu = 0, 1, 2, 3$, with the coordinate $x^4 \equiv y$, $-L \leq y \leq L$ parameterizing the fifth dimension, is defined by the action

$$S = S_g + S_{\phi+SM}, \quad (1)$$

where S_g and $S_{\phi+SM}$ are given by

$$S_g = -2M^3 \int d^4x \int_{-L}^L dy R \sqrt{g}, \quad (2)$$

$$S_{\phi+SM} = \int d^4x \int_{-L}^L dy \left(\frac{1}{2} g^{MN} \partial_M \phi \partial_N \phi - V(\phi) \right) \sqrt{g} \quad (3)$$

$$- \int_{y=0} \sqrt{-\tilde{g}} V_1(\phi) d^4x + \int_{y=L} \sqrt{-\tilde{g}} (-V_2(\phi) + L_{SM}) d^4x.$$

Here the signature of the metric g_{MN} is chosen to be $(+, -, -, -, -)$, M is the fundamental five-dimensional energy scale, $V(\phi)$ is a bulk scalar field potential, $V_{1,2}(\phi)$ are brane scalar field potentials, $\tilde{g} = \det \tilde{g}_{\mu\nu}$, and $\tilde{g}_{\mu\nu}$ denotes the metric induced on the branes. The space of extra dimension is the orbifold S^1/Z_2 , which is realized as the circle of circumference $2L$ with the points y and $-y$ identified. Correspondingly, the metric g_{MN} and the scalar field ϕ satisfy the orbifold symmetry conditions

$$g_{\mu\nu}(x, -y) = g_{\mu\nu}(x, y), \quad g_{\mu 4}(x, -y) = -g_{\mu 4}(x, y), \quad (4)$$

$$g_{44}(x, -y) = g_{44}(x, y), \quad \phi(x, -y) = \phi(x, y).$$

The branes are located at the fixed points of the orbifold, $y = 0$ and $y = L$, and it is assumed that the SM fields with Lagrangian L_{SM} live on the brane at $y = L$.

For this form of the action, the vacuum solution for gravity and the stabilizing scalar field and the vacuum solution for the SM fields are independent. If we consider this brane-world model to be an indivisible theory, it is reasonable to believe that there should be a common interconnected vacuum solution for all these fields. To this end, let us modify action (3) so that it contains a quartic interaction of the stabilizing scalar field and of the Higgs field, which would connect the stabilization of the extra dimension size and the SM spontaneous symmetry breaking:

$$S_{\phi+SM} = \int d^4x \int_{-L}^L dy \left(\frac{1}{2} g^{MN} \partial_M \phi \partial_N \phi - V(\phi) \right) \sqrt{g} \quad (5)$$

$$- \int_{y=0} \sqrt{-\tilde{g}} V_1(\phi) d^4x + \int_{y=L} \sqrt{-\tilde{g}} (-V_2(\phi) + L_{SM-HP} + L_{int}(\phi, H)) d^4x,$$

where the Lagrangian L_{SM-HP} is the SM Lagrangian without the Higgs potential, which is replaced by the interaction Lagrangian

$$L_{int}(\phi, H) = -\lambda \left(|H|^2 - \frac{\xi}{M} \phi^2 \right)^2, \quad (6)$$

ξ being a positive dimensionless parameter. A similar interaction Lagrangian quadratic in the stabilizing scalar field was discussed in [18].

The background solutions for the metric and the scalar field, which preserve the Poincaré invariance in any four-dimensional subspace $y = const$, look like

$$\begin{aligned} ds^2 &= e^{-2A(y)} \eta_{\mu\nu} dx^\mu dx^\nu - dy^2 \equiv \gamma_{MN}(y) dx^M dx^N, & (7) \\ \phi(x, y) &= \phi(y), & (8) \end{aligned}$$

with $\eta_{\mu\nu}$ denoting the flat Minkowski metric, whereas the background (vacuum) solution for the Higgs field is standard,

$$H_{vac} = \begin{pmatrix} 0 \\ \frac{v}{\sqrt{2}} \end{pmatrix}, \quad (9)$$

with all the other SM fields being equal to zero.

If one substitutes this ansatz into the equations corresponding to action (1), one gets a relation between the vacuum value of the Higgs field and the value of the field ϕ on the brane at $y = L$,

$$\phi^2(L) = \frac{Mv^2}{2\xi}. \quad (10)$$

This means that in such a scenario the Higgs field vacuum expectation value, being proportional to the value of the stabilizing scalar field on the TeV brane, arises dynamically as a result of the gravitational bulk stabilization.

The gravitational background solution follows from the well-known system of nonlinear differential equations for functions $A(y), \phi(y)$ [6],

$$\begin{aligned} \frac{dV}{d\phi} + \frac{dV_1}{d\phi} \delta(y) + \frac{dV_2}{d\phi} \delta(y - L) &= -4A' \phi' + \phi'' & (11) \\ 12M^3 (A')^2 + \frac{1}{2} (V - \frac{1}{2}(\phi')^2) &= 0 \\ \frac{1}{2} (\frac{1}{2}(\phi')^2 + V + V_1 \delta(y) + V_2 \delta(y - L)) &= -2M^3 (-3A'' + 6(A')^2) \quad , \end{aligned}$$

where the first equation is the equation for the scalar field and the other two follow from the Einstein equations. Here $' = d/dy$.

Suppose we have a solution $A(y), \phi(y)$ to this system for an appropriate choice of the parameters of the potentials such that the interbrane distance is stabilized and equal to L . This means that the vacuum energy of the scalar field has a minimum for this value of the interbrane distance.

Now the linearized theory is obtained by representing the metric, the scalar and the Higgs

field in the unitary gauge as

$$g_{MN}(x, y) = \gamma_{MN}(y) + \frac{1}{\sqrt{2M^3}} h_{MN}(x, y), \quad (12)$$

$$\phi(x, y) = \phi(y) + \frac{1}{\sqrt{2M^3}} f(x, y), \quad (13)$$

$$H(x) = \begin{pmatrix} 0 \\ \frac{v+\sigma(x)}{\sqrt{2}} \end{pmatrix}, \quad (14)$$

substituting this representation into action (1) and keeping the terms of the second order in h_{MN} , f and σ . The Lagrangian of this action is the standard free Lagrangian of the SM (i.e., the masses of all the SM fields, except the Higgs field, are expressed in the same way as usual in terms of the vacuum value of the Higgs field and the coupling constants) together with the standard second variation Lagrangian of the stabilized Randall-Sundrum model [4] supplemented by an interaction term of fields f and σ . The part of the Lagrangian relevant to the Higgs-radion mixing is

$$\left[-\frac{1}{2M^3} \left(\frac{1}{2} \frac{d^2 V_2}{d\phi^2} + \frac{2\lambda v^2 \xi}{M} \right) f^2 + \frac{2\lambda v^2 \sqrt{\xi}}{M^2} f\sigma - \frac{1}{2} 2\lambda v^2 \sigma^2 \right] \delta(y-L). \quad (15)$$

The bulk scalar field f can be expanded in KK modes. In the case under consideration we can, in the standard way, find the equations for the mass spectrum and the wave functions of the KK excitations of the scalar fields just by replacing $\frac{1}{2} \frac{d^2 \lambda_2}{d\phi^2} \rightarrow \frac{1}{2} \frac{d^2 V_2}{d\phi^2} + \frac{2\lambda v^2 \xi}{M}$ in the formulas of paper [4] (we note that in this paper the signature of the metric was $(-, +, +, +, +)$, and for this reason some formulas of that paper may differ in sign from the corresponding formulas in the present paper). Namely, in this paper it was shown that it was most convenient to describe the scalar degrees of freedom of stabilized brane-world models by the field $\chi = e^{-2A(y)} h_{44}(x, y)$ related to the field f by the gauge condition

$$f = -3M^3 \frac{e^{2A}}{\phi'} \chi'. \quad (16)$$

The equations of motion and the boundary conditions on the branes for the field χ define wave functions $\{\chi_n(y)\}$, corresponding to mass eigenvalues μ_n^2 . Expanding the field f in these modes, substituting this expansion into the second variation Lagrangian and integrating over the extra dimension coordinate y , we get a four-dimensional Lagrangian, in which there is an interaction between the modes and the Higgs field coming from the term $\frac{2\lambda v^2 \sqrt{\xi}}{M^2} f\sigma$. Using gauge condition (16), the mode decomposition of $\chi(x, y)$,

$$\chi(x, y) = \sum_{n=0}^{\infty} \phi_n(x) \chi_n(y),$$

and the boundary condition for the mode wave function $\chi_n(y)$ at $y=L$ [4] rewritten in terms of eq. (15),

$$\left(\frac{1}{2} \frac{d^2 V_2}{d\phi^2} + \frac{\phi''}{\phi'} + \frac{2\lambda v^2 \xi}{M} \right) \chi'_n - \mu_n^2 e^{2A} \chi_n|_{y=L} = 0,$$

the field f can be expressed through $\chi_n(y)$ as follows:

$$\frac{f(x, L)}{3M^3} = -\frac{\chi' e^{2A}}{\phi'} \Big|_{y=L} = -\frac{\chi'}{\phi'} \Big|_{y=L} = -\sum_{n=1}^{\infty} \frac{\mu_n^2}{\left(\frac{1}{2} \frac{d^2 V_2}{d\phi^2} + \frac{\phi''}{\phi'} + \frac{2\lambda v^2 \xi}{M}\right) \phi'} \chi_n(L) \phi_n(x),$$

where we have taken into account that $A(L) = 0$ in order to have Galilean coordinates on the brane at $y = L$ [3].

Thus, the couplings of the modes to the Higgs field can be written as

$$\sum_{n=1}^{\infty} \mu_n^2 a_n \phi_n(x) \sigma(x),$$

where we have introduced dimensionless quantities

$$-\frac{6\lambda M v^2 \sqrt{\xi}}{\left(\frac{1}{2} \frac{d^2 V_2}{d\phi^2} + \frac{\phi''}{\phi'} + \frac{2\lambda v^2 \xi}{M}\right) \phi'} \chi_n(L) = a_n, \quad (17)$$

which are supposed to be positive.

These couplings are proportional to the squared masses of the modes and can be rather large for large n . Below we will see that it is the dimensionless quantities a_n that are of importance. They are proportional to the values of the wave functions of the modes on the brane and it is convenient to express them in terms of the ratios of the latter and a_1 :

$$a_n = a_1 \alpha_n, \quad \alpha_n = \frac{\chi_n(L)}{\chi_1(L)}. \quad (18)$$

These ratios must go to zero for large n in order for the cumulative effect of the radion KK tower to be finite. In paper [4] the scalar wave functions $\{\chi_n(y)\}$ have been found explicitly in a stabilized brane-world model, where the warp factor is approximately equal to that of the unstabilized Randall-Sundrum model, and one can check that the quantities a_n are indeed positive and the ratios α_n really fall off fairly quickly for large n in this case. It is rather difficult to find them explicitly in the stabilized brane-world models, where the warp factor is different from the exponential of a linear function, as it is in the Randall-Sundrum model. A study of such stabilized brane-world models has been carried out in papers [3, 4], and it was found that they may also solve the hierarchy problem of the gravitational interaction, giving rise to the masses of KK excitations in the TeV energy range. However, the corresponding equations cannot be solved exactly and should be studied numerically for each set of the fundamental parameters of the model, which is a very complicated and laborious task.

Here, we will not carry out such calculations for a specific stabilized brane-world model, but rather give a qualitative description of the phenomena due to the interaction of the Higgs field with the radion and its KK tower, choosing the masses and the coupling constants in a consistent manner and taking into account the present-day theoretical and experimental restrictions on their values.

3 Higgs-radion mixing and the effective Lagrangian

The part of the extended SM Lagrangian containing the scalar fields linearly or quadratically looks like

$$\begin{aligned}
L_{part} &= \frac{1}{2}\partial_\mu\sigma\partial^\mu\sigma - \frac{1}{2}2\lambda v^2\sigma^2 + \frac{1}{2}\sum_{n=1}^{\infty}\partial_\mu\phi_n\partial^\mu\phi_n - \frac{1}{2}\sum_{n=1}^{\infty}\mu_n^2\phi_n^2 \\
&+ \sum_{n=1}^{\infty}\mu_n^2 a_n\phi_n\sigma - \sum_f \frac{m_f}{v}\bar{\psi}_f\psi_f\sigma - \sum_{n=1}^{\infty}b_n\phi_n(T_\mu^\mu + \Delta T_\mu^\mu) \\
&+ \frac{2M_W^2}{v}W_\mu^-W^{\mu+}\sigma + \frac{M_Z^2}{v}Z_\mu Z^\mu\sigma + \frac{M_W^2}{v^2}W_\mu^-W^{\mu+}\sigma^2 + \frac{M_Z^2}{2v^2}Z_\mu Z^\mu\sigma^2,
\end{aligned} \tag{19}$$

where T_μ^μ is the trace of the SM energy-momentum tensor and ΔT_μ^μ is the conformal anomaly of massless vector fields explicitly given by

$$\Delta T_\mu^\mu = \frac{\beta(g_s)}{2g_s}G_{\rho\sigma}^{ab}G_{ab}^{\rho\sigma} + \frac{\beta(e)}{2e}F_{\rho\sigma}F^{\rho\sigma} \tag{20}$$

with β being the well-known QCD and QED β functions.

The coupling of the scalar modes to the trace of the energy-momentum tensor comes from the standard interaction Lagrangian for the metric fluctuations [4], which results in the expression for the parameters b_n in terms of the scalar mode wave functions:

$$b_n = \frac{1}{2\sqrt{8M^3}}\chi_n(L). \tag{21}$$

In the case of the lowest scalar mode, the radion, this parameter is usually denoted as

$$b_1 = \frac{1}{\Lambda_r}, \tag{22}$$

where Λ_r is supposed to be of the order of the fundamental energy scale M . Below we will use Λ_r as a natural scale for the interactions of the radion and for those induced by its KK tower. For this reason, it is also convenient to express b_n in terms of Λ_r and α_n defined in (18) as

$$b_n = \frac{\alpha_n}{\Lambda_r}. \tag{23}$$

In what follows, we consider the phenomenology of the Higgs boson and the radion in the energy range much lower than the masses of the radion excitations. In this case, we can pass to a low-energy approximation for this Lagrangian by dropping the kinetic terms of the radion excitation fields and integrating them out, which gives the following effective Lagrangian for the interactions of the Higgs and radion fields with the SM fields

$$\begin{aligned}
L_{part-eff} &= \frac{1}{2}\partial_\mu\sigma\partial^\mu\sigma - \frac{1}{2}(2\lambda v^2 - d^2)\sigma^2 + \frac{1}{2}\partial_\mu\phi_1\partial^\mu\phi_1 - \frac{1}{2}\mu_1^2\phi_1^2 + \mu_1^2 a_1\phi_1\sigma \\
&- \frac{1}{\Lambda_r}\phi_1(T_\mu^\mu + \Delta T_\mu^\mu) - \frac{c}{\Lambda_r}\sigma(T_\mu^\mu + \Delta T_\mu^\mu) - \sum_f \frac{m_f}{v}\bar{\psi}_f\psi_f\sigma \\
&+ \frac{2M_W^2}{v}W_\mu^-W^{\mu+}\sigma + \frac{M_Z^2}{v}Z_\mu Z^\mu\sigma + \frac{M_W^2}{v^2}W_\mu^-W^{\mu+}\sigma^2 + \frac{M_Z^2}{2v^2}Z_\mu Z^\mu\sigma^2,
\end{aligned} \tag{24}$$

where the new parameters are defined in terms of the old ones as follows:

$$d^2 = a_1^2 \sum_{n=2}^{\infty} \mu_n^2 \alpha_n^2, \quad c = a_1 \sum_{n=2}^{\infty} \alpha_n^2. \quad (25)$$

We have already mentioned that these series should be convergent. The positive parameter d^2 can be of the order of v^2 , because the mass term $2\lambda v^2 - d^2$ should be positive, and, within the approach under consideration, the coupling constant of the Higgs boson self-interaction λ can be larger than in the regular SM case. Possible restrictions on the parameters c will be discussed below.

Next we turn to the mass matrix of the fields σ and ϕ_1 , which looks like

$$\mathcal{M} = \begin{pmatrix} 2\lambda v^2 - d^2 & -\frac{1}{2}\mu_1^2 a_1 \\ -\frac{1}{2}\mu_1^2 a_1 & \mu_1^2 \end{pmatrix}. \quad (26)$$

This matrix can be diagonalized by a rotation matrix

$$\mathcal{R}^T \mathcal{M} \mathcal{R} = \text{diag}(m_h^2, m_r^2), \quad \mathcal{R} = \begin{pmatrix} \cos \theta & -\sin \theta \\ \sin \theta & \cos \theta \end{pmatrix},$$

where the rotation angle θ is defined by the relation

$$\tan 2\theta = \frac{\mu_1^2 a_1}{\mu_1^2 - 2\lambda v^2 + d^2}. \quad (27)$$

It is not difficult to see that it is sufficient to take this angle only in the interval $-\pi/4 < \theta < \pi/4$, which is one full period of the function $\tan 2\theta$.

The observable masses of the mass eigenstates are given by the expressions

$$\begin{aligned} m_h^2 &= 2\lambda v^2 - d^2 - \frac{\mu_1^2 - 2\lambda v^2 + d^2}{2} \left(\sqrt{1 + \frac{4a_1^2}{(\mu_1^2 - 2\lambda v^2 + d^2)^2}} - 1 \right) \\ m_r^2 &= \mu_1^2 + \frac{\mu_1^2 - 2\lambda v^2 + d^2}{2} \left(\sqrt{1 + \frac{4a_1^2}{(\mu_1^2 - 2\lambda v^2 + d^2)^2}} - 1 \right), \end{aligned}$$

which are written in the form that explicitly shows that the smaller mass becomes smaller and the larger one becomes larger due to the mixing. The latter, in particular, means that the observable masses m_r^2 and m_h^2 cannot be exactly equal in the presence of the mixing and the mixing angle θ is negative for $m_r^2 < m_h^2$ in accordance with the observation in paper [6].

The original unobservable parameters of the matrix \mathcal{M} can be expressed in terms of the observable parameters m_h^2 , m_r^2 and θ . The correspondence between these sets of parameters is one-to-one, if one puts the mixing angle $\theta = 0$ for $m_h^2 = m_r^2$. Then the following formula for the parameter a_1 can be easily obtained:

$$a_1 = \frac{(m_r^2 - m_h^2) \sin 2\theta}{m_r^2 \cos^2 \theta + m_h^2 \sin^2 \theta}.$$

This formula, together with the second formula in (25), gives an expression for the parameter c in terms of the physical masses and the mixing angle

$$c = \frac{(m_r^2 - m_h^2) \sin 2\theta}{m_r^2 \cos^2 \theta + m_h^2 \sin^2 \theta} \left(\sum_{n=2}^{\infty} \alpha_n^2 \right) \quad (28)$$

which also depends on the sum of the wave function ratios α_n^2 . These ratios are, of course, model dependent, and, although they should fall off with n in order for the sum to be convergent, one cannot exclude that, in certain models, several first ratios can be of the order of unity. Thus, one can conservatively estimate this sum to be also of the order of unity,¹ which gives the estimate for the parameter c

$$0 < c < c_{max} = \frac{(m_r^2 - m_h^2) \sin 2\theta}{m_r^2 \cos^2 \theta + m_h^2 \sin^2 \theta}, \quad (29)$$

which will be used in the subsequent calculations.

The physical mass eigenstate fields $h(x), r(x)$ are easily expressed in terms of matrix \mathcal{R} and the original fields as

$$\begin{aligned} h(x) &= \cos \theta \sigma(x) + \sin \theta \phi_1(x) \\ r(x) &= -\sin \theta \sigma(x) + \cos \theta \phi_1(x). \end{aligned} \quad (30)$$

The field $h(x)$ is called the Higgs-dominated field, and the field $r(x)$ is called the radion-dominated field because $\cos \theta > |\sin \theta|$ in the interval $-\pi/4 < \theta < \pi/4$ (we recall that $\theta < 0$ for $m_r^2 < m_h^2$). The interaction of these fields with the fields of the Standard Model is given by the following effective Lagrangian:

$$\begin{aligned} L_{h-r} &= \frac{1}{2} \partial_\mu h \partial^\mu h - \frac{1}{2} m_h^2 h^2 + \frac{1}{2} \partial_\mu r \partial^\mu r - \frac{1}{2} m_r^2 r^2 \\ &- \frac{(c \cos \theta + \sin \theta)}{\Lambda_r} h (T_\mu^\mu + \Delta T_\mu^\mu) + \frac{(c \sin \theta - \cos \theta)}{\Lambda_r} r (T_\mu^\mu + \Delta T_\mu^\mu) \\ &- \sum_f \frac{m_f}{v} \bar{\psi}_f \psi_f (\cos \theta h - \sin \theta r) + \frac{2M_W^2}{v} W_\mu^- W^{\mu+} (\cos \theta h - \sin \theta r) \\ &+ \frac{M_Z^2}{v} Z_\mu Z^\mu (\cos \theta h - \sin \theta r) + \frac{M_W^2}{v^2} W_\mu^- W^{\mu+} (\cos \theta h - \sin \theta r)^2 \\ &+ \frac{M_Z^2}{2v^2} Z_\mu Z^\mu (\cos \theta h - \sin \theta r)^2. \end{aligned} \quad (31)$$

The effective four-dimensional interaction Lagrangian (31) expressed in terms of the physical Higgs-dominated $h(x)$ and radion-dominated $r(x)$ fields contains their interactions with the SM fields and involves only five parameters in addition to those of the SM²: the masses of the Higgs-dominated and radion-dominated fields m_h and m_r , the mixing angle θ , the (inverse) coupling

¹For example, in the stabilized model discussed in paper [4], the approximate wave functions of the scalar modes give rather rough estimates for the value of this sum in the interval (0.02, 0.2) for the radion mass in the interval $100 \text{ GeV} < m_r < 500 \text{ GeV}$ and the mass of its first KK excitation of the order of 1 TeV.

²We do not assume *a priori* with which state, the Higgs-dominated or the radion-dominated, the 125-GeV boson observed at the LHC is associated.

constant of the radion to the trace of the energy-momentum tensor of the SM fields Λ_r and the parameter c that accommodates the contributions of the integrated-out heavy scalar modes. We would like to note here that, according to formulas (28) and (29), the parameter c is proportional to its maximal value c_{max} and therefore depends on the masses m_h , m_r and the mixing angle θ , which is a particular feature of the model.

It is interesting to examine what occurs to Lagrangian (31) if the fundamental energy scale M goes to infinity. In the model under consideration, it is impossible just to take the limit $M \rightarrow \infty$ because there exists relation (10) for the model parameters, which includes the vacuum value of the Higgs field. In the stabilized brane-world model discussed in [4], the radion mass was found to be proportional to $\phi^2(L)/M^3$. Thus, in order to keep this mass fixed, we have to take the limit $M \rightarrow \infty$ and $\xi \rightarrow 0$ so that $M^2\xi = const$. One can see that in this case a_1 , which is proportional to $M\sqrt{\xi}$, does not vanish, whereas Λ_r defined in (21) and (22) goes to infinity. As a result, in Lagrangian (31) the terms with the energy-momentum tensor that are proportional to $1/\Lambda_r$ vanish, but all the other terms remain because the mixing angle must not be equal to zero. The situation in this case is rather similar to the one in the SM extended by an extra singlet scalar [19, 20]. However, there are differences due to extra interactions between the Higgs field and the singlet scalar in these models, arising from the scalar field potentials that are absent in our model.

We would also like to note here that, if we formally put the parameters a_1 , c and θ equal to zero, i.e., consider the case of the zero mixing, Lagrangian (31) becomes just the SM Higgs Lagrangian plus the usual Lagrangian of the radion interaction with the SM fields via the trace of the SM energy-momentum tensor. In the case of a nonzero mixing, there are additional terms in this Lagrangian that may lead to certain changes in the collider phenomenology of the Higgs boson and the radion. These issues will be discussed in the next section.

4 Phenomenological constraints from the LHC

The effective Lagrangian (31) describes the interactions of the Higgs-dominated $h(x)$ and the radion-dominated $r(x)$ fields with the Standard Model fields and with each other. A few natural questions arise. What model parameter regions are allowed by the present-day experimental data such as LEP and Tevatron searches, Higgs-like 125-GeV boson discovery and the Higgs signal strength measurements at various signatures at the LHC, and the limits from searches for the second Higgs-like boson at the LHC? Is an interpretation of the observed boson as a radion-dominated state is still possible for some model parameters?

Detailed answers to such questions require a corresponding detailed phenomenological analysis, which will be considered in a separate study. In this paper we present constraints coming from the discovery of a 125-GeV Higgs-like boson at the LHC, measurements of the signal strengths at various production channels and decay modes, and searches for heavier Higgs bosons.

The Feynman rules needed for our study can be easily derived from Lagrangian (31) and are given in the table in the Appendix. We have omitted the terms coming from off-shell fermions since the corresponding contributions to physical processes are exactly canceled out by additional diagrams with contact four-point vertices coming from the first-order expansions in gauge couplings of the SM energy-momentum tensor trace as was proved in [21].

The Feynman rules have been implemented as a “new model” in a special version of the CompHEP code [22, 23, 24] which also includes a routine for χ^2 analysis of the Higgs signal strength in a way similar to those used in papers [25, 26]. The next-to-next-to-leading order (NNLO) corrections are taken into account in the CompHEP computations and in the corresponding analysis by multiplying the involved vertices by correction factors for each model parameter point such that the partial and the total SM Higgs decay widths and the Higgs production cross sections in gluon-gluon fusion (GGF) are exactly equal to those presented by the LHC Higgs Cross Section Working Group [27, 28]. Because of the similarity of the Higgs boson and the radion production and decay amplitudes including loops [21], the same correction factors have been used for the Higgs- and the radion-dominated states.

We examine two possible scenarios, where the observed 125-GeV boson is either the Higgs-dominated state or the radion-dominated state.

4.1 Higgs-dominated state at 125 GeV

In order to understand how much room is left for the radion-dominated state, we first demonstrate various decay and production properties of this state. In Fig. 1, the decay branching ratios for the radion-dominated boson are shown as functions of its mass.

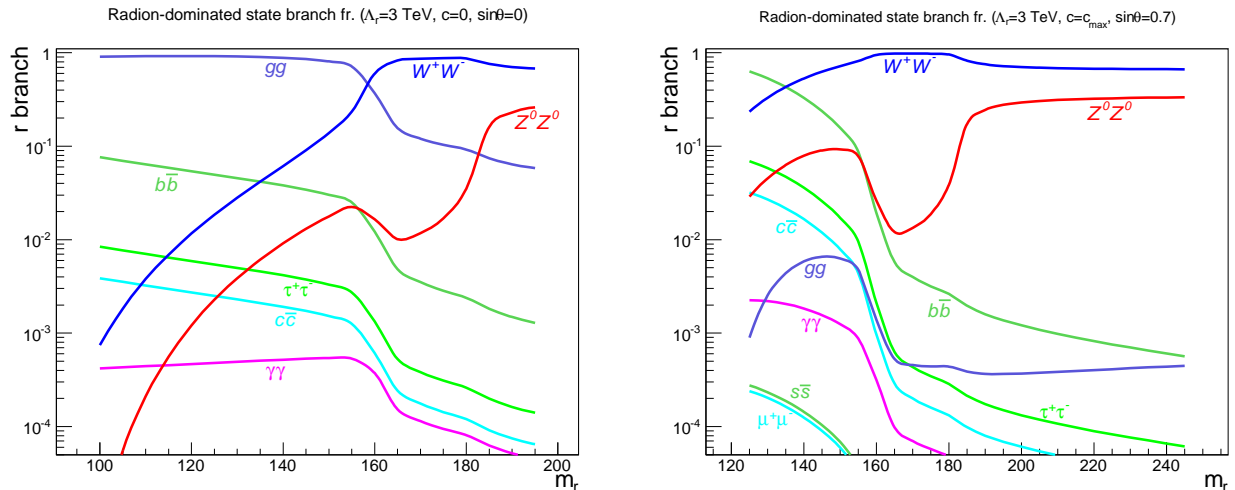


Figure 1: Radion-dominated state branching ratios as functions of m_r ($m_h = 125 \text{ GeV}$, $\Lambda_r = 3 \text{ TeV}$). The left plot corresponds to $\sin \theta = 0$ and $c = 0$; the right plot corresponds to $\sin \theta = 0.7$, and c is equal to its maximum value c_{max} .

The left plot shows the well-known branching behavior [29] of the radion without mixing with the Higgs boson and interacting with the SM fields only via the trace of the energy-momentum tensor. As is well known, the main decay mode of the light radion is the decay to two gluons due to the anomaly enhancement. However, once the mixing with the Higgs boson is included, the picture might be changed drastically because of the appearance of Higgs-like couplings for the radion-dominated state proportional to $\sin \theta$ and because of the influence of the higher scalar modes encoded in the parameter c .

In Fig. 2, the behavior of the upper level of this parameter as a function of the radion mass and the mixing angle is illustrated. We recall that for $\theta > 0$ the radion-dominated state is

heavier than the Higgs-dominated state, $m_r > m_h$, and vice versa ($\theta < 0$ for $m_r < m_h$), and therefore, for $\theta < 0$, $m_r > m_h$ and for $\theta > 0$, $m_r < m_h$, the areas shown as zero plates are not allowed. If one takes a rather large mixing angle, for example, $\sin \theta = 0.7$, the $b\bar{b}$ decay mode is dominating as shown in Fig. 1 on the right plot. Because of a compensation in the gluon-gluon-radion vertex between the trace anomaly part proportional to $1/\Lambda_r$ and the mentioned Higgs-like part proportional to $\sin \theta/v$ the vertex can be very small for some particular regions of the parameter space. This leads to an interesting feature shown in Fig. 1 that the decay branching ratio for the radion-dominated state to two gluons may be smaller than the branching ratio to two photons. Because of the mentioned compensations between various parts of the

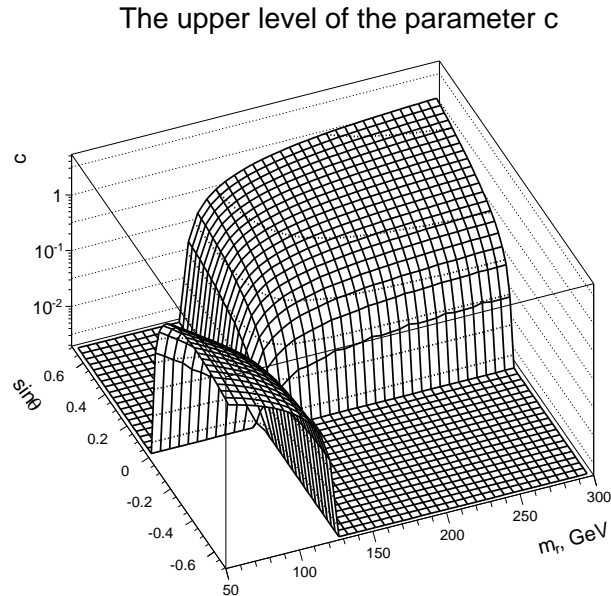


Figure 2: Two-dimensional plot of the upper level c_{max} of the parameter c as a function of $(m_r, \sin \theta)$.

interaction vertex of the radion-dominated state with gluons, the behavior of the total width and the production cross sections for $\gamma\gamma$ and ZZ^* modes in gluon-gluon fusion also have some minima, as one can see from Figs. 3 and 4. From the cross sections one gets the corresponding signal strengths for the radion-dominated state divided by the SM Higgs cross sections. In our analysis we use the Higgs signal strengths for all the channels, as given recently by the CMS [30] and ATLAS [31] collaborations. As a result of the standard χ^2 analysis, one gets the regions in the parameter space (the mass of the radion-dominated state and the mixing angle with the Higgs boson) which are still allowed. The regions allowed either by considering only the $\gamma\gamma$ mode, and the $\gamma\gamma$ together with the ZZ^* modes are given in the left and the right plots of Fig. 5, correspondingly, for a not-too-large mass range for the radion-dominated state. For both cases, all the main production processes [GGF, vector boson fusion (VBF), and associated production with vector bosons (VH) and with the top quarks (ttH)] are taken into account. The interference effects of the Higgs- and radion-dominated states are also taken into account, which is especially important in the case of close resonances. The contours in all figures correspond to 65%, 90% and 99% best-fit confidence level (CL) regions with $\Delta\chi^2$ less

than 2.10, 4.61 and 9.21, respectively, which is the standard presentation of two-parameter fits and was used in earlier papers (see, e.g., [25, 32]). Thus, the dark shaded area corresponds to 65% CL of the fit, the medium shaded area corresponds to 90% CL of the fit, and the light shaded area corresponds to 99% CL of the fit.

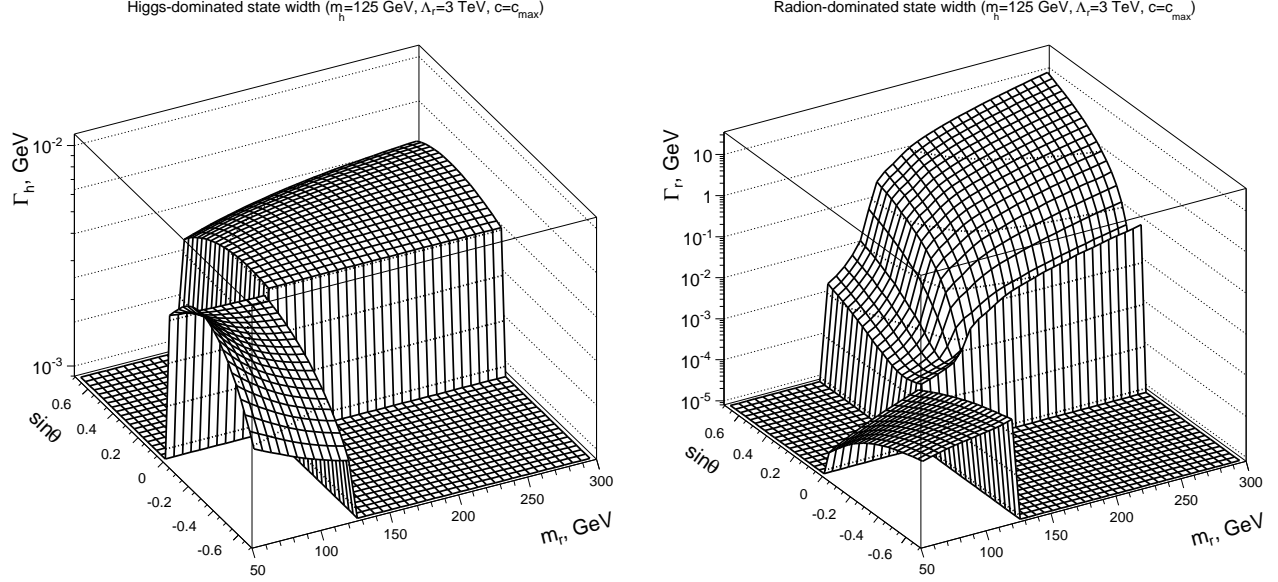


Figure 3: Three-dimensional plots of the total width as a function of $(m_r, \sin\theta)$ for the LHC at $\sqrt{s} = 8$ TeV and $m_h = 125$ GeV, $\Lambda_r = 3$ TeV, $c = c_{max}$. The left plot corresponds to the Higgs-dominated state $h(x)$, and the right plot corresponds to the radion-dominated state $r(x)$.

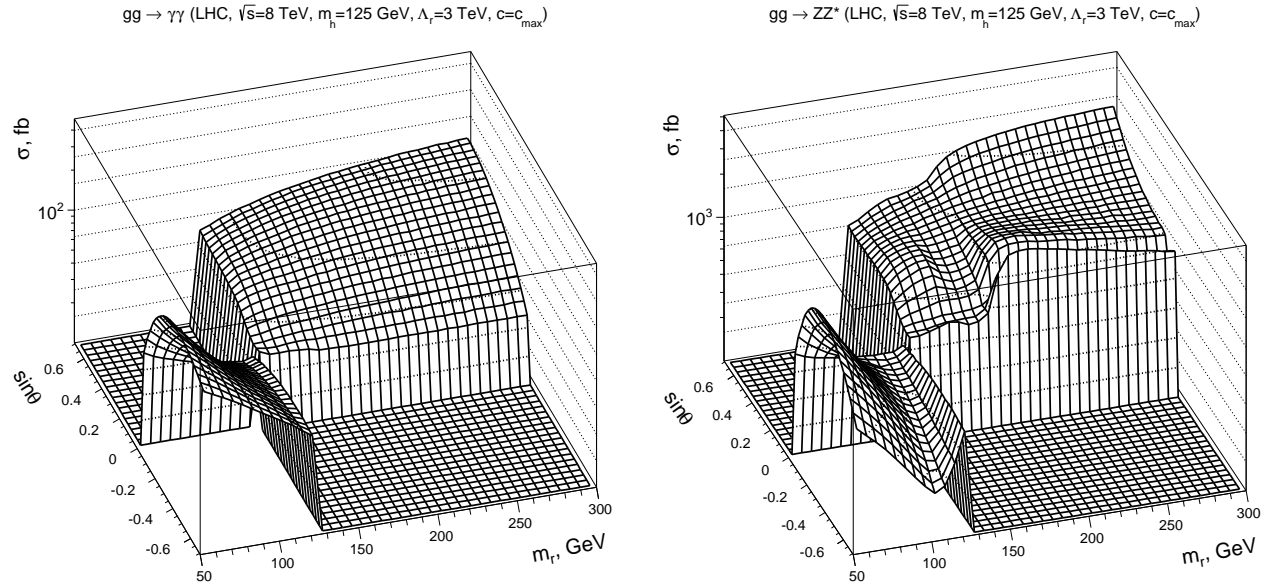


Figure 4: Three-dimensional plots of the partial cross section as a function of $(m_r, \sin\theta)$ for the LHC at $\sqrt{s} = 8$ TeV and $m_h = 125$ GeV, $\Lambda_r = 3$ TeV, $c = c_{max}$. The left plot corresponds to the $gg \rightarrow \gamma\gamma$ channel, and the right plot corresponds to the $gg \rightarrow ZZ^*$ channel.

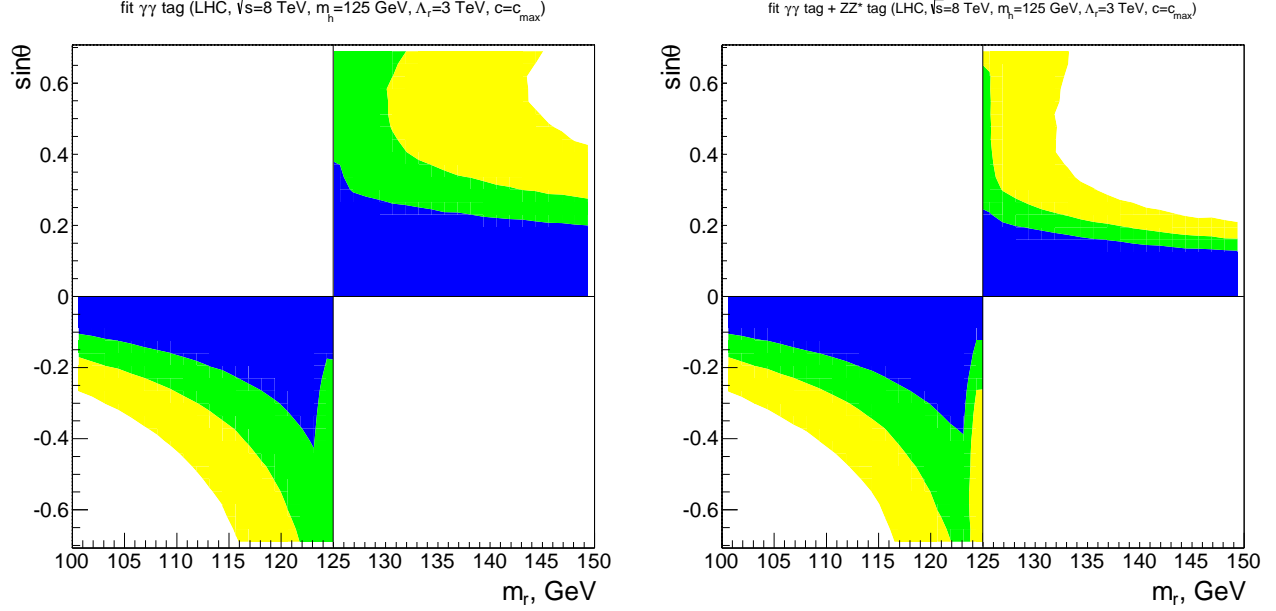


Figure 5: Exclusion contours for the partial χ^2 fit in the $(m_r, \sin\theta)$ plane for the LHC at $\sqrt{s} = 8\text{TeV}$ and $m_h = 125\text{GeV}$, $\Lambda_r = 3\text{TeV}$, $c = c_{max}$. The dark, medium and light shaded areas correspond to 65%, 90% and 99% CL of the fit, respectively. The left plot corresponds to the $pp \rightarrow \gamma\gamma$ channel, and the right plot corresponds to the combined fit of the $pp \rightarrow \gamma\gamma$ and $pp \rightarrow ZZ^*$ channels.

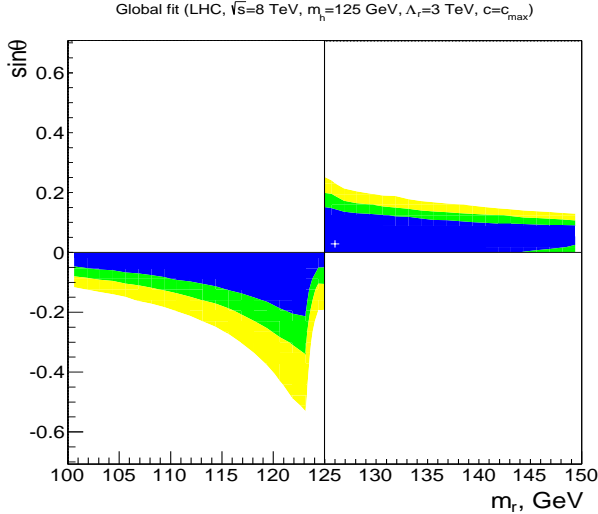


Figure 6: Exclusion contours for the combined χ^2 fit in the $(m_r, \sin\theta)$ plane, which includes all the production processes (GGF, VBF, VH and ttH) and all the main decay channels ($\gamma\gamma, ZZ^*, WW^*, b\bar{b}, \tau^+\tau^-$) for the LHC at $\sqrt{s} = 8\text{TeV}$ and $m_h = 125\text{GeV}$, $\Lambda_r = 3\text{TeV}$, $c = c_{max}$. The dark, medium and light shaded areas correspond to 65%, 90% and 99% CL of the fit, respectively. The white cross marks the best-fit point.

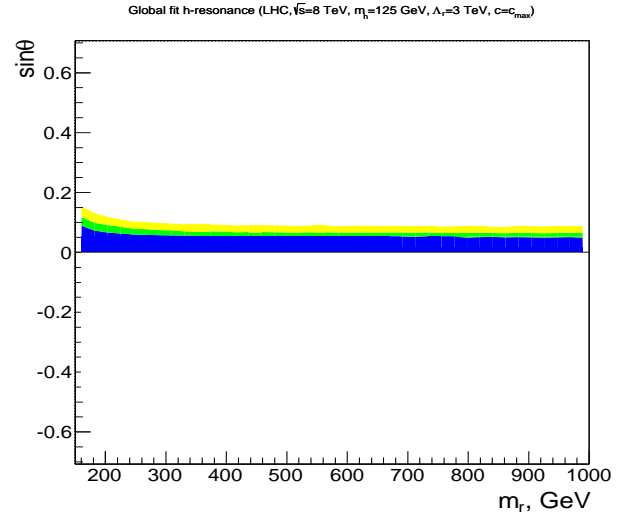


Figure 7: Exclusion contours in the heavy radion mass parameter for the combined χ^2 fit in the $(m_r, \sin\theta)$ plane that comes from the signal strengths at 125 GeV for all the production processes (GGF, VBF, VH and ttH) and all the main decay channels ($\gamma\gamma, ZZ^*, WW^*, b\bar{b}, \tau^+\tau^-$) for the LHC at $\sqrt{s} = 8\text{TeV}$ and $m_h = 125\text{GeV}$, $\Lambda_r = 3\text{TeV}$, $c = c_{max}$. The dark, medium and light shaded areas correspond to 65%, 90% and 99% CL of the fit, respectively.

In Fig. 5, one can see that the $\gamma\gamma$ mode alone allows the presence of the radion-dominated state for masses both below and above the 125 GeV. The ZZ^* mode gives some additional restrictions on the parameter space especially in the mass region closer to the Z-boson pair threshold, where the cross section is increased. When all the modes are taken into account, the allowed parameter space region is reduced further, which is shown in Fig. 6.

For larger values of the radion mass, the influence of this parameter on 125-GeV signal strength is very small, resulting in the allowed area shown in Fig. 7. However, in the case of a large resonance mass region, one has to take into account the exclusion limits given very recently by the CMS [33] and ATLAS [34] collaborations, coming from searches for heavy Higgs bosons. If the radion-dominated state has a large mass, it would contribute as a resonance in this region.

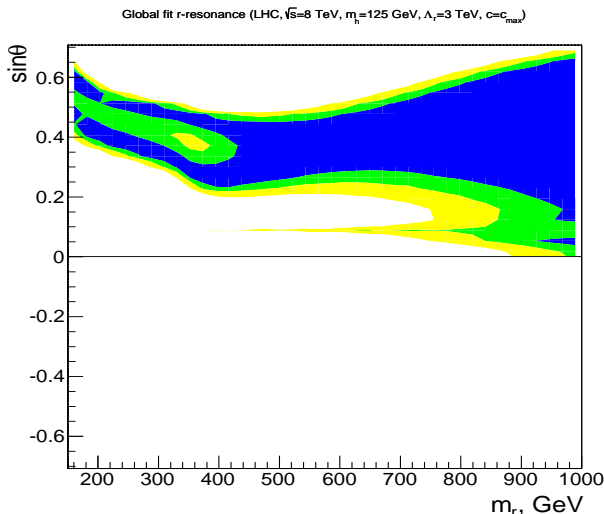


Figure 8: Exclusion contours in the heavy radion mass parameter for the combined χ^2 fit of the CMS and ATLAS exclusion regions at a high mass range by the resonance production and decay of the radion-dominated state with corresponding heavy mass in the $(m_r, \sin \theta)$ plane. The dark, medium and light shaded areas correspond to 65%, 90% and 99% CL of the fit, respectively.

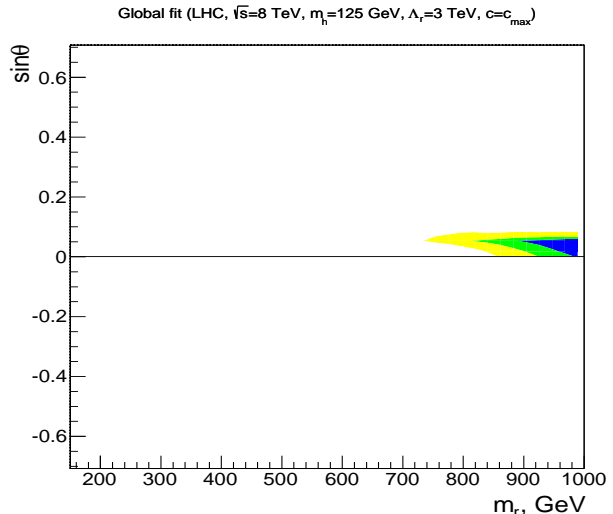


Figure 9: The region in the $(m_r, \sin \theta)$ still allowed by the common fit of the CMS and ATLAS exclusion limits for heavy Higgs searches and restrictions from the fit of the influence of those parameters on the signal strengths at the point 125 GeV. The dark, medium and light shaded areas correspond to 65%, 90% and 99% CL of the fit, respectively.

From the comparison of the radion cross section computation and the experimental limits by CMS and ATLAS by performing the corresponding χ^2 fit, one gets a rather large allowed area in the $(m_r, \sin \theta)$ parameter plane, as shown in Fig. 8. When taken together, fits of the data from both the signal strengths and from the direct searches for heavy Higgs resonances significantly restrict the allowed region for the heavy radion mass to a small area at very high masses, as demonstrated in Fig. 9.

Obviously, if one considers larger values of the parameter Λ_r , the cross section of the radion-dominated state gets smaller and the allowed region for such a state is increased. This is demonstrated in Fig. 10, where the parameter Λ_r is chosen to be 5 GeV with all the other parameters being the same as for the considered 3-TeV case.

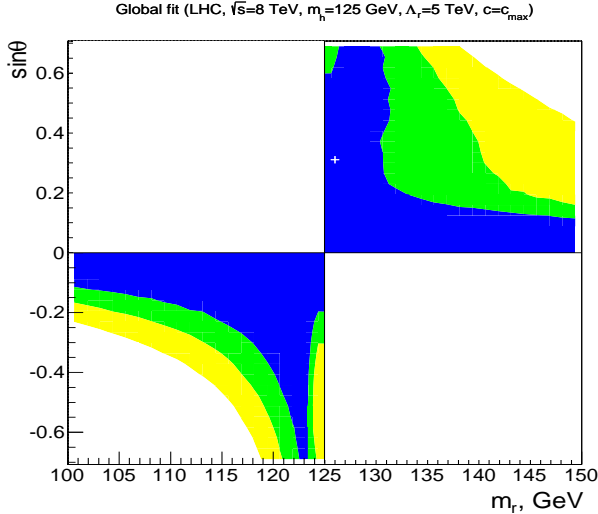


Figure 10: Exclusion contours for the combined χ^2 fit in the $(m_r, \sin\theta)$ plane that includes all the production processes (GGF, VBF, VH and ttH) and all the main decay channels ($\gamma\gamma, ZZ^*, WW^*, b\bar{b}, \tau^+\tau^-$) for the LHC at $\sqrt{s} = 8\text{TeV}$ and $m_h = 125\text{GeV}$, $\Lambda_r = 5\text{TeV}$, $c = c_{max}$. The dark, medium and light shaded areas correspond to 65%, 90% and 99% CL of the fit, respectively. The white cross marks the best-fit point.

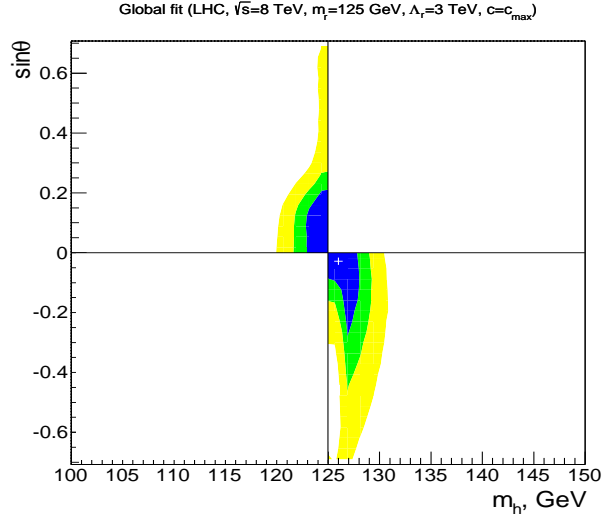


Figure 11: Exclusion contours for the combined χ^2 fit in the $(m_h, \sin\theta)$ plane that comes from the signal strengths at 125 GeV for all the production processes (GGF, VBF, VH and ttH) and all the main decay channels ($\gamma\gamma, ZZ^*, WW^*, b\bar{b}, \tau^+\tau^-$) for the LHC at $\sqrt{s} = 8\text{TeV}$ and $m_r = 125\text{GeV}$, $\Lambda_r = 3\text{TeV}$, $c = c_{max}$. The dark, medium and light shaded areas correspond to 65%, 90% and 99% to CL of the fit, respectively. The white cross marks the best-fit point.

4.2 Radion-dominated state at 125 GeV

Now let us consider briefly the case where the radion-dominated state has mass 125 GeV, and, using the same analysis strategy, find the regions for the mass of the Higgs-dominated state and the mixing angle allowed by two signal strengths. For this case, we have carried out all the corresponding calculations and have drawn the plots similar to those in Figs. 2–7, which we will not present here for the sake of brevity. We only dwell upon the result of the χ^2 analysis that is presented in Fig. 11.

As one can see, such a scenario is strongly disfavored in comparison with the previous case. The mass of the Higgs-dominated state might still be very close to the mass of the radion-dominated state in a wide range of mixing angle. Such a possibility exists in both scenarios.

5 Conclusion

In the present paper we have considered the Higgs-radion mixing arising in stabilized brane-world models due to merging the mechanism of stabilization of the extra dimension size and the Higgs mechanism of spontaneous symmetry breaking on the TeV brane. We have discussed phenomenological restrictions on model parameters coming from coupling measurements and searches for heavy bosons at the LHC. This mixing is, of course, similar in many aspects to the one arising due to the Higgs-curvature term on the brane. However, an important difference is the presence of an extra coupling at low energies of the Higgs-dominated field to the trace of

the SM energy-momentum tensor originating from the coupling of this field to the heavy scalar states of the radion KK tower.

In order to study the physical consequences of the Higgs-radion mixing in stabilized brane-world models, we derived the effective Lagrangian and gave a qualitative description of the phenomena, taking consistent values for the masses, the coupling constants, and the mixing angle, which are useful for comparing the results of our calculations with the experimental data at the LHC. It turned out that, though the interaction of an individual higher excited scalar state with the Higgs field may be weak, their cumulative effect on the Higgs-radion mixing may be observable. If they give noticeable contributions to the parameter c , it leads to certain changes in the collider phenomenology of the Higgs boson. A similar contribution of the directly unobservable higher tensor KK modes to scattering processes was discussed in [35].

In the framework of this model, we have studied two *a priori* possible scenarios: The scalar state discovered at 125 GeV is either a Higgs-dominated state or a radion-dominated state. In our analysis, we used measurements of the 125-GeV Higgs signal strengths by the ATLAS and CMS collaborations and exclusion limits obtained in searches for heavy Higgs-like states. Our results show that the interpretation of the 125-GeV scalar state as a Higgs-dominated state is the preferred one, although the radion component in this state can be rather large. Depending on the value of the radion coupling constant Λ_r , the allowed regions for the mass of the radion-dominated state have been found. It turns out that the radion-dominated state can either have a mass close to 125 GeV or a mass close to the TeV range. The allowed regions somewhat increase with the growth of the radion coupling constant Λ_r .

We have also shown that the interpretation of the 125-GeV scalar state as a radion-dominated state is not completely excluded by the two leading signal strength measurements, though in this case the restrictions on the allowed masses of the Higgs-dominated state are very stringent. The mass of the Higgs-dominated state can be close to 125 GeV, which is in accordance with our analysis of this state at 125 GeV. Thus, in the considered model the presence of two nearly degenerate states close to 125 GeV is a very probable scenario.

6 Acknowledgements

The work was supported by Grant No. 14-12-00363 of the Russian Science Foundation.

7 Appendix: Feynman rules

In Table 1, the constants and the functions of the momenta are explicitly given by the following expressions: $b_{QCD} = 7$, $b_2 = \frac{19}{6}$, $b_Y = -\frac{41}{6}$, $C_h = \sin \theta + c \cdot \cos \theta$, $C_r = \cos \theta - c \cdot \sin \theta$, $F_W = -(2 + 3y_W + 3y_W(2 - y_W)f(y_W))$, $F_t = y_t(1 + (1 - y_t)f(y_t))$, $y_i = 4m_i^2/(2p_1 \cdot p_2)$,

$$f(z) = \begin{cases} \left[\sin^{-1} \left(\frac{1}{\sqrt{z}} \right) \right]^2, & z \geq 1 \\ -\frac{1}{4} \left[\log \frac{1+\sqrt{1-z}}{1-\sqrt{1-z}} - i\pi \right]^2, & z < 1. \end{cases}$$

Triple vertices	Feynman rules
$\bar{t} \quad t \quad h$	$-M_t \cdot \left(\frac{C_h}{\Lambda_r} + \frac{\cos \theta}{v} \right)$
$\bar{t} \quad t \quad r$	$-M_t \cdot \left(\frac{C_r}{\Lambda_r} - \frac{\sin \theta}{v} \right)$
$Z_\mu \quad Z_\nu \quad h$	$2 \cdot M_Z^2 \cdot \left(\frac{C_h}{\Lambda_r} + \frac{\cos \theta}{v} \right) \cdot g^{\mu\nu}$
$Z_\mu \quad Z_\nu \quad r$	$2 \cdot M_Z^2 \cdot \left(\frac{C_r}{\Lambda_r} - \frac{\sin \theta}{v} \right) \cdot g^{\mu\nu}$
$W_\mu^+ \quad W_\nu^- \quad h$	$2 \cdot M_W^2 \cdot \left(\frac{C_h}{\Lambda_r} + \frac{\cos \theta}{v} \right) \cdot g^{\mu\nu}$
$W_\mu^+ \quad W_\nu^- \quad r$	$2 \cdot M_W^2 \cdot \left(\frac{C_r}{\Lambda_r} - \frac{\sin \theta}{v} \right) \cdot g^{\mu\nu}$
$G_\mu \quad G_\nu \quad h$	$\frac{g_s^2}{8\pi^2} \cdot \left[b_{QCD} \cdot \frac{C_h}{\Lambda_r} + F_t \cdot \left(\frac{C_h}{\Lambda_r} + \frac{\cos \theta}{v} \right) \right] \cdot (g^{\mu\nu} p_1 p_2 - p_1^\nu p_2^\mu)$
$G_\mu \quad G_\nu \quad r$	$\frac{g_s^2}{8\pi^2} \cdot \left[b_{QCD} \cdot \frac{C_r}{\Lambda_r} + F_t \cdot \left(\frac{C_r}{\Lambda_r} - \frac{\sin \theta}{v} \right) \right] \cdot (g^{\mu\nu} p_1 p_2 - p_1^\nu p_2^\mu)$
$A_\mu \quad A_\nu \quad h$	$\frac{e^2}{8\pi^2} \cdot \left[(b_2 + b_Y) \cdot \frac{C_h}{\Lambda_r} + (F_W + \frac{8}{3} F_t) \cdot \left(\frac{C_h}{\Lambda_r} + \frac{\cos \theta}{v} \right) \right] \cdot (g^{\mu\nu} p_1 p_2 - p_1^\nu p_2^\mu)$
$A_\mu \quad A_\nu \quad r$	$\frac{e^2}{8\pi^2} \cdot \left[(b_2 + b_Y) \cdot \frac{C_r}{\Lambda_r} + (F_W + \frac{8}{3} F_t) \cdot \left(\frac{C_r}{\Lambda_r} - \frac{\sin \theta}{v} \right) \right] \cdot (g^{\mu\nu} p_1 p_2 - p_1^\nu p_2^\mu)$

Table 1: Triple vertices.

References

- [1] W. D. Goldberger and M. B. Wise, Phys. Rev. Lett. **83**, 4922 (1999) [hep-ph/9907447].
- [2] O. DeWolfe, D. Z. Freedman, S. S. Gubser and A. Karch, Phys. Rev. D **62**, 046008 (2000) [hep-th/9909134].
- [3] E. E. Boos, Y. S. Mikhailov, M. N. Smolyakov and I. P. Volobuev, Nucl. Phys. B **717**, 19 (2005) [hep-th/0412204].
- [4] E. E. Boos, Y. S. Mikhailov, M. N. Smolyakov and I. P. Volobuev, Mod. Phys. Lett. A **21**, 1431 (2006) [hep-th/0511185].
- [5] G. F. Giudice, R. Rattazzi and J. D. Wells, Nucl. Phys. B **595**, 250 (2001) [hep-ph/0002178].
- [6] C. Csaki, M. L. Graesser and G. D. Kribs, Phys. Rev. D **63**, 065002 (2001) [hep-th/0008151].
- [7] G. Aad *et al.* [ATLAS Collaboration], Phys. Lett. B **716**, 1 (2012) [arXiv:1207.7214]; S. Chatrchyan *et al.* [CMS Collaboration], Phys. Lett. B **716**, 30 (2012) [arXiv:1207.7235].
- [8] Z. Chacko, R. Franceschini and R. K. Mishra, JHEP **1304**, 015 (2013) [arXiv:1209.3259].
- [9] Z. Chacko, R. K. Mishra and D. Stolarski, JHEP **1309**, 121 (2013) [arXiv:1304.1795].
- [10] H. Kubota and M. Nojiri, Phys. Rev. D **87**, 076011 (2013) [arXiv:1207.0621].

- [11] G. C. Cho, D. Nomura and Y. Ohno, *Mod. Phys. Lett. A* **28**, 1350148 (2013) [arXiv:1305.4431].
- [12] N. Desai, U. Maitra and B. Mukhopadhyaya, *JHEP* **1310**, 093 (2013) [arXiv:1307.3765].
- [13] P. Cox, A. D. Medina, T. S. Ray and A. Spray, *JHEP* **1402**, 032 (2014) [arXiv:1311.3663].
- [14] M. Geller, S. Bar-Shalom and A. Soni, *Phys. Rev. D* **89**, 095015 (2014) [arXiv:1312.3331].
- [15] D. W. Jung and P. Ko, *Phys. Lett. B* **732**, 364 (2014) [arXiv:1401.5586].
- [16] S. Bhattacharya, M. Frank, K. Huitu, U. Maitra, B. Mukhopadhyaya and S. K. Rai, *Phys. Rev. D* **91**, 016008 (2015) [arXiv:1410.0396].
- [17] H. Davoudiasl, J. L. Hewett and T. G. Rizzo, *JHEP* **0308**, 034 (2003) [hep-ph/0305086].
- [18] I. Volobuev, *PoS QFTHEP 2011*, 054 (2013).
- [19] S. I. Godunov, A. N. Rozanov, M. I. Vysotsky and E. V. Zhemchugov, arXiv:1503.01618 [hep-ph].
- [20] T. Robens and T. Stefaniak, *Eur. Phys. J. C* **75** (2015) 104 [arXiv:1501.02234 [hep-ph]].
- [21] E. Boos, S. Keizerov, E. Rahmetov and K. Svirina, *Phys. Rev. D* **90**, 095026 (2014) [arXiv:1409.2796].
- [22] E. Boos *et al.* [CompHEP Collaboration], *Nucl. Instrum. Meth. A* **534**, 250 (2004) [hep-ph/0403113].
- [23] E. Boos, V. Bunichev, M. Dubinin, L. Dudko, V. Edneral, V. Ilyin, A. Kryukov and V. Savrin *et al.*, *PoS ACAT 08*, 008 (2008) [arXiv:0901.4757].
- [24] E. Boos, V. Bunichev and M. Dubinin, *PoS QFTHEP 2013*, 015 (2013).
- [25] E. Boos, V. Bunichev, M. Dubinin and Y. Kurihara, *Phys. Rev. D* **89**, 035001 (2014) [arXiv:1309.5410].
- [26] E. Boos, V. Bunichev, M. Dubinin and Y. Kurihara, *Phys. Lett. B* **739**, 410 (2014) [arXiv:1402.4143].
- [27] S. Dittmaier *et al.* [LHC Higgs Cross Section Working Group Collaboration], arXiv:1101.0593.
- [28] S. Heinemeyer *et al.* [LHC Higgs Cross Section Working Group Collaboration], arXiv:1307.1347.
- [29] K. -m. Cheung, *Phys. Rev. D* **63**, 056007 (2001) [hep-ph/0009232];
- [30] V. Khachatryan *et al.* [CMS Collaboration], *Eur. Phys. J. C* **75** (2015) 5, 212 [arXiv:1412.8662 [hep-ex]].
- [31] G. Aad *et al.* [ATLAS Collaboration], arXiv:1507.04548 [hep-ex].

- [32] J. R. Espinosa, C. Grojean, M. Muhlleitner and M. Trott, JHEP **1205**, 097 (2012) [arXiv:1202.3697].
- [33] V. Khachatryan *et al.* [CMS Collaboration], arXiv:1504.00936 [hep-ex].
- [34] G. Aad *et al.* [ATLAS Collaboration], arXiv:1507.05930 [hep-ex].
- [35] E. E. Boos, V. E. Bunichev, M. N. Smolyakov and I. P. Volobuev, Phys. Rev. D **79**, 104013 (2009) [arXiv:0710.3100].